

THE METHOD OF ENVELOPE CURRENTS FOR RAPID SIMULATION OF WEAKLY NONLINEAR COMMUNICATIONS CIRCUITS

Vuk Borich, Jack East, George Haddad

EECS Department, the University of Michigan, Ann Arbor
e-mail: vborich@engin.umich.edu

ABSTRACT

The method of *Envelope Currents* is introduced as an efficient tool for simulation of circuits in weakly nonlinear operating regimes. The approach is aimed at spectral regrowth analyses of circuits excited by narrowband-modulated digital carriers. Starting from the method of Nonlinear Currents, and using the condition of narrowband excitation, we show that circuit equations reduce to systems of linear ordinary differential equations in the complex envelopes of the node voltages. Time-integration of the resulting equations reduces to a sequence of solutions of sparse triangular systems, and is therefore very efficient. The paper concludes with a circuit example.

1. INTRODUCTION

Modern wireless communications systems employ varying envelope modulation formats that suffer in-band distortion, known as *spectral regrowth*, when processed by nonlinear circuits such as amplifiers and mixers [1]. Accurate determination of spectral regrowth is of great interest to circuit designers. Although behavioral methods offer quick estimates of nonlinear distortion, circuit-level approaches are generally considered as more accurate [2]. The main difficulty in applying circuit simulation techniques to digitally-modulated carriers is the fundamental requirement to simulate long pulse sequences in order to reduce run-to-run variations of the simulation results; the requirement is rooted in the random nature of digital data. Consequently, a large number of frequency components must be taken into account in the case of frequency-domain simulation techniques; likewise, circuit equations must be integrated over long time periods in the case of time-domain techniques.

Several methods for nonlinear circuit simulation suitable for modulated carrier excitations have been proposed. They include multitone harmonic balance [8][9] and hybrid time-frequency [3]-[7] methods. Despite the advances, simulation times are relatively long because of the above-mentioned, fundamental limitations. For example, spectral regrowth simulation of a single-stage amplifier requires at least one minute per power point on a modern workstation.

Often, circuit behavior may be considered *weakly nonlinear*. Examples include low-noise, quasilinear transmitter, and instrumentation amplifiers. When a circuit is weakly nonlinear, the available methods [3]-[9] invariably converge faster than in the strongly nonlinear case, as a result of fewer iterations and lower

sampling rates. However, the mild nonlinear behavior is not exploited directly and the improvement in speed is modest.

In this paper, we present the method of Envelope Currents, a technique rooted in the method of Nonlinear Currents [10][11], that offers significant speed improvements by taking advantage of the weakly nonlinear assumption. It may be viewed as an efficient extension of the method of Nonlinear Currents to digitally modulated excitations. After reviewing the method of Nonlinear Currents in Section 2 and 3, Section 4 presents the theoretical foundations of the Envelope Current algorithm. We conclude the paper by a circuit example and a discussion on the implications of the weakly nonlinear assumption in Sections 5 and 6.

NOMENCLATURE

Time domain variables are in lowercase and frequency domain variables are in uppercase; bold type is used for matrix-valued variables; tilde sign denotes a signal's complex envelope; subscripts are carrier frequency or nonlinear order indices; time-sample indices are enclosed in brackets; *left* superscripts denote iteration counts; n is the order of a nonlinear term, m is the time-sample index, and l denotes iteration counts.

For example, ${}^l\tilde{v}_n[m]$ is the m^{th} sample of the envelope of that component of the l^{th} iterate of the node voltage vector which is centered at the n^{th} carrier harmonic.

2. CIRCUIT MODELS

We consider circuits consisting of voltage-controlled charges and conductors, and linear lumped and distributed elements. Nonlinear element equations are expanded in power series of the controlling voltages as:

$$g(v) = \sum_{n=1}^N g_n v^n, \quad (1)$$

for nonlinear conductors controlled by a single voltage, and

$$g(v, u) = \sum_{m, n: 0 < n+m \leq N} g_{mn} v^m u^n, \quad (2)$$

in the case of two control voltages. Similar expansions are used for nonlinear charge elements. In this paper, $N = 3$. The series coefficients are evaluated at the DC bias point which is assumed constant as a consequence of mild nonlinearity. We consider the linear ($m + n = 1$) terms in expansions (1) and (2) to be ordinary lumped linear elements. The collection of all linear elements, including the linear terms in (1) and (2), will be referred to as the *linear subcircuit*.

This research is supported by the DDRE Multidisciplinary University Research Initiative (MURI) and managed by the ARO under grant DAAH04-96-1-0377.

3. THE METHOD OF NONLINEAR CURRENTS

Let the circuit of Section 2 be driven by arbitrary sources represented by their Norton equivalents. Assume that the quiescent point has been calculated and that the expansion coefficients in (1) and (2) have been determined. Further, short-circuit all DC voltage sources, and open-circuit all DC current sources.

Select the node voltages as a convenient set of unknown circuit variables. By the method of Nonlinear Currents [10][11], the unknown voltage vector is given by

$$\mathbf{v} = {}^0\mathbf{v} + \sum_{l=1}^L {}^l\mathbf{v} \quad (3)$$

where ${}^0\mathbf{v}$ is the DC solution and ${}^l\mathbf{v}$ solves

$$L[{}^l\mathbf{v}] = {}^l\mathbf{i}, \quad l = 1, 2, \dots, L. \quad (4)$$

$L[\]$ symbolically denotes the system of integrodifferential equations obtained by nodal analysis of the linear subcircuit. The source current vector ${}^l\mathbf{i}$ arises from the l^{th} order "nonlinear current" sources defined as follows:

1. The first order ($l = 1$) nonlinear current sources are the original driving sources.
2. To obtain the second order ($l = 2$) nonlinear current sources, each nonlinear conductor is replaced by an equivalent current source given by

$$g_2({}^1v)^2, \quad \text{or}$$

$$g_{20}({}^1v)^2 + g_{11}({}^1v)({}^1u) + g_{02}({}^1u)^2,$$

depending on the number of controlling voltages. The expressions for the nonlinear charge elements are similar, i.e.,

$$\frac{d}{dt}c_2({}^1v)^2, \quad \text{or}$$

$$\frac{d}{dt}[c_{20}({}^1v)^2 + c_{11}({}^1v)({}^1u) + c_{02}({}^1u)^2].$$

1v and 1u are the controlling voltages for the nonlinear element as calculated from the first-order solution, and g_{mn} and c_{mn} are the expansion coefficients from (1) and (2).

3. The third order sources are given by

$$g_3({}^1v)^3 + 2g_2({}^1v)({}^2v), \quad \text{or}$$

$$\begin{aligned} &g_{30}({}^1v)^3 + g_{03}({}^1u)^3 + g_{21}({}^1v)^2({}^1u) + g_{12}({}^1u)^2({}^1v) \\ &+ 2g_{20}({}^1v)({}^2v) + 2g_{02}({}^1u)({}^2u) \\ &+ g_{11}({}^1v)({}^2u) + g_{11}({}^2v)({}^1u), \end{aligned}$$

and analogous expressions are used for capacitive elements. Again, 1v and 1u are the controlling voltages as calculated from the lower order solutions. In this paper, the order of the Nonlinear Current algorithm is restricted to $L = 3$.

4. THE METHOD OF ENVELOPE CURRENTS

Let the driving sources be narrowband-modulated signals of the form

$$i_s(t) = Re\{\tilde{i}_s(t)e^{j\omega_c t}\} \quad (5)$$

and let us apply the method of Nonlinear Currents as described in Section 3. Because of the excessive ratio of the carrier and envelope bandwidth, direct time-domain integration of (4) is, at best, very inefficient; instead, we seek a different approach.

With (5) as the driving source, at any step of the Nonlinear Current algorithm (4), all circuit variables, call them $x'(t)$, take the general form

$$x'(t) = Re\left\{\sum_{n=0}^N \tilde{x}_n(t)e^{jn\omega_c t}\right\}. \quad (6)$$

Since the components of $x'(t)$ centered at $-\omega_c, \dots, -N\omega_c$ are complex conjugates of those centered at $\omega_c, \dots, N\omega_c$, we represent the circuit variables as complex signals of the form

$$x(t) = \sum_{n=0}^N \tilde{x}_n(t)e^{jn\omega_c t}, \quad (7)$$

with the frequency-domain representation

$$X(\omega) = \sum_{n=0}^N \tilde{X}_n(\omega - n\omega_c). \quad (8)$$

For spectral regrowth analyses, it is convenient to approximate (7) by quasiperiodic signals, i.e., to represent each complex envelope $\tilde{x}_n(t)$ by a finite number of discrete sinusoids. For the case of digitally modulated signals, the envelopes are approximated as periodic signals with long time periods; a Fourier series representation of the envelope and its substitution in (7) yield the desired quasiperiodic representation.

In quasiperiodic steady-state, and with (8) in mind, the Nonlinear Current method (4) has a frequency-domain equivalent

$$\mathbf{Y}(\omega) {}^l\tilde{\mathbf{V}}_n(\omega - n\omega_c) = {}^l\tilde{\mathbf{I}}_n(\omega - n\omega_c) \quad (9)$$

$$l = 1, \dots, L, \quad n = 0, \dots, N,$$

$\mathbf{Y}(\omega)$ being the node-admittance matrix of the linear subcircuit.

In principle, (9) can be solved for the unknown ${}^l\tilde{\mathbf{V}}_n(\omega - n\omega_c)$. As in the case of direct time-integration, this is an inefficient approach. Recall that the envelopes must be sampled over long time periods, usually several hundred data pulses, resulting in a representation by as many as several thousand frequency components. Then, a rigorous approach would require the evaluation and factorization of $\mathbf{Y}(\omega)$ at thousands of frequency points. Hence, the frequency domain solution (9) would not be significantly faster than [9], which is a more general approach.

However, notice that the spectra of the circuit waveforms in (8) exist only in narrow bands near $n\omega_c$. So, consider the first-order Taylor series expansion of $\mathbf{Y}(\omega)$ about $n\omega_c$:

$$\mathbf{Y}(\omega) = \mathbf{Y}(n\omega_c) + \mathbf{\Omega}_n \mathbf{Y}'(n\omega_c), \quad (10)$$

where $\mathbf{\Omega}_n = \text{diag}(\omega - n\omega_c)$. Higher order expansions are straightforward. If (10) is substituted in (9), an inverse Fourier transform of (9) yields:

$$\mathbf{Y}(n\omega_c) {}^l\tilde{\mathbf{v}}_n(t) - j\mathbf{Y}'(n\omega_c) \frac{d}{dt} {}^l\tilde{\mathbf{v}}_n(t) = {}^l\tilde{\mathbf{i}}_n(t), \quad (11)$$

$$l = 1, \dots, L, \quad n = 0, \dots, N.$$

Equation (11) constitutes the Envelope Current algorithm. For each l and n , (11) is a system of ordinary linear differential equations in the complex envelopes of the node voltages. When $L = N = 3$ there are twelve such systems, but some of them have zero solutions, and others are not of interest. In the end, a total of four systems need to be solved.

The "envelope currents" on the right hand side of (11) are obtained by substituting in Steps 1-3 of Section 3 the assumed form of the node voltages (6), and collecting the terms at center frequency $n\omega_c$.

In case of nonlinear conductors controlled by a single voltage, for example, this procedure yields

$$\begin{aligned} {}^2\tilde{i}_0 &= \frac{g_2}{2} |{}^1\tilde{v}_1|^2 \\ {}^2\tilde{i}_2 &= \frac{g_2}{2} ({}^1\tilde{v}_1)^2 \\ {}^3\tilde{i}_1 &= \frac{3g_3}{4} ({}^1\tilde{v}_1)^2 ({}^1\tilde{v}_1^*) + 2g_2 ({}^1\tilde{v}_1) ({}^2\tilde{v}_0) \\ &\quad + g_2 ({}^1\tilde{v}_1^*) ({}^2\tilde{v}_2) \end{aligned}$$

and for nonlinear charges

$$\begin{aligned} {}^2\tilde{i}_0 &= \frac{c_2}{2} \frac{d}{dt} (|{}^1\tilde{v}_1|^2) \\ {}^2\tilde{i}_2 &\approx j\omega_c c_2 ({}^1\tilde{v}_1)^2 \\ {}^3\tilde{i}_1 &\approx j3\omega_c \left[\frac{3c_3}{4} ({}^1\tilde{v}_1)^2 ({}^1\tilde{v}_1^*) + 2c_2 ({}^1\tilde{v}_1) ({}^2\tilde{v}_0) \right. \\ &\quad \left. + c_2 ({}^1\tilde{v}_1^*) ({}^2\tilde{v}_2) \right] \end{aligned}$$

To solve (11), sample the envelope waveforms at M points over the interval $(M-1)\Delta t$, where Δt is a suitably chosen, fixed time step. The Backward-Euler [12] discretization method, for example, results in the update rule

$$\begin{aligned} [j\mathbf{Y}'(n\omega_c) - \Delta t\mathbf{Y}(n\omega_c)]^l \tilde{\mathbf{v}}_n[m+1] = \\ j\mathbf{Y}'(n\omega_c)^l \tilde{\mathbf{v}}_n[m] - \Delta t^l \tilde{\mathbf{i}}_n[m+1], \end{aligned} \quad (12)$$

$${}^l\tilde{\mathbf{v}}_{n,0} = \mathbf{0},$$

$$l = 1, \dots, L, \quad n = 0, \dots, N.$$

Higher order integration formulas can be employed with similar results, as long as the time step Δt is constant. The (highly sparse) coefficient matrices $j\mathbf{Y}'(n\omega_c) - \Delta t\mathbf{Y}(n\omega_c)$ are factorized once for all at the beginning of the iteration process. Observe that only four such matrices need to be stored and factorized. Hence, once the coefficient matrices are factorized, nearly all of the simulation time is spent on solving sparse triangular linear systems. These steps can be implemented efficiently, resulting in a dramatic increase in simulation speed over the existing circuit simulation techniques.

The unwanted transient component in (11) can be handled heuristically in two ways. We may force the envelope waveform to start at zero with no loss of accuracy or generality in distortion studies; since the envelope waveform is slow-rising, and since the pulse sequence is usually long, the transient component likely introduces negligible errors in spectral regrowth calculations. A safer alternative is to introduce several "dummy" pulses for the purpose of integrating out the transient component, with a small price in overall simulation time.

The memory requirements are controlled mainly by the storage of the node voltage waveforms ${}^l\tilde{\mathbf{v}}_n[m]$ and the envelope currents ${}^l\tilde{\mathbf{i}}_n[m]$. Five such (complex) waveforms must be stored. In double precision, the third-order ($N = L = 3$) Envelope Current method requires approximately $80KM$ bytes of memory, where K is the number of nodes, and M the number of time samples. Note, however, that the memory requirements can be relaxed – only those node voltage waveforms that control the nonlinear elements, and those that the user wishes to analyze, need to be stored. In that case, the required memory is considerably smaller than $80KM$ bytes.

5. EXAMPLE

The Envelope Current method has been implemented in a user-oriented, in-house simulator. An example 5 GHz power amplifier circuit, shown in Fig. 1, has been investigated. In Fig. 1, the nonlinear capacitors are described by junction formulas, and the nonlinear transconductance is described by the Statz model. A narrowband QPSK signal shown in Fig. 2 was applied to the input. The distorted output is shown in Fig. 3. With 512 data symbols and 32 samples per symbol, the simulation requires approximately 5 seconds on a Sun ULTRA10 workstation.

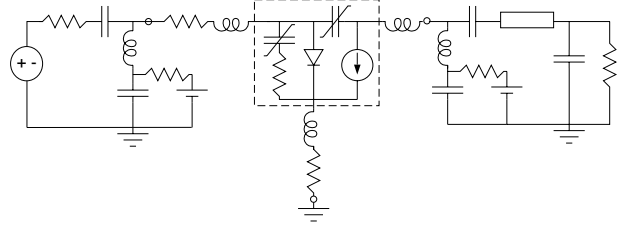


Figure 1: Test Circuit.

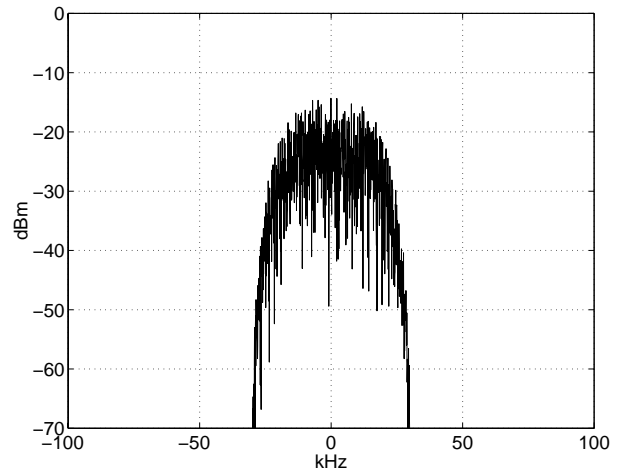


Figure 2: Input Spectrum.

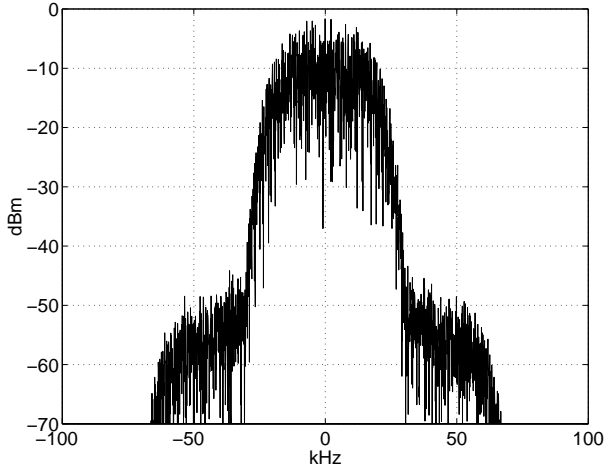


Figure 3: Output Spectrum.

6. DYNAMIC RANGE LIMITATIONS

Because of the assumed weakly nonlinear behavior, the dynamic range of the method is of immediate concern. To illustrate the limitations, a two-tone signal was applied to the amplifier of Fig. 1. Two tone signals are handled easily by the proposed method, by setting $\tilde{i}_s(t) = A \sin[(\omega_2 - \omega_1)t]$ in (5), where ω_2 and ω_1 are the angular frequencies of the two tones. The results were compared to an in-house harmonic-balance simulator based on [9], and the results are shown in Fig. 3. At lower power levels, the methods are in excellent agreement. As the peaks of the drain current enter the linear or cutoff regions, gain begins to compress, and the power series expansions that were used in the saturation region, do not adequately describe the device behavior. For this reason, the model was changed at the knee of the gain compression curve by performing a least squares fit of the device equations to (1) and (2) over the entire operating region. Alternatively, fifth order expansions in (1) and (2) would extend the dynamic range of the method and achieve closer agreement with harmonic-balance simulations at the expense of more than two-fold increase in simulation speed and memory requirements.

7. SUMMARY

A new method has been presented for weakly nonlinear circuit simulation under digitally-modulated carrier excitations. Dramatic improvements in simulation speed have been achieved by taking direct advantage of the mild nonlinear behavior. Starting from the method of Nonlinear Currents, the circuit equations are formulated as systems of linear differential equations in the complex envelopes of the node voltages. The majority of the simulation time is spent on solving sparse triangular systems resulting in rapid simulation runs. A spectral regrowth study of a single-stage amplifier has been presented. The simulation required approximately 5 seconds on a modern workstation.

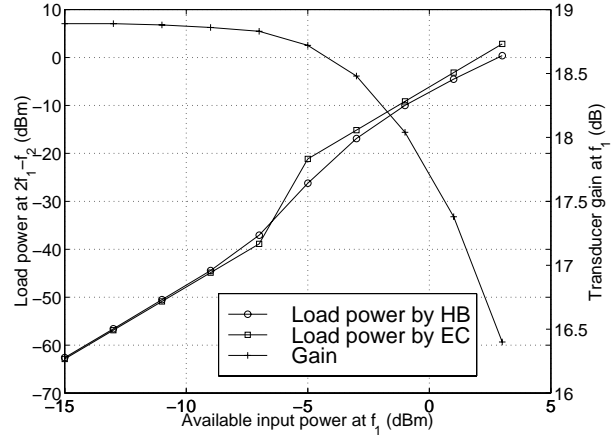


Figure 4: Comparison with Harmonic Balance.

8. REFERENCES

- [1] S. Kenney and A. Leke, "Power amplifier spectral regrowth for digital cellular and PCS applications," *Microwave Journal*, pp. 74-90, Oct. 1995.
- [2] J. Sevic and J. Staudinger, "Simulation of adjacent channel power for digital wireless communication systems," *Microwave Journal*, pp. 68-80, Oct. 1996.
- [3] V. Rizzoli, *et al.*, "A modulation-oriented piecewise harmonic-balance technique suitable for transient analysis and digitally modulated signals," *Proc. EuMC*, pp. 546-549, 1996.
- [4] E. Ngoya and R. Larcheveque, "Envelope transient analysis: a new method for the transient and steady state analysis of microwave communication circuits and systems," *1996 MTT-S Digest*, pp. 1365-1368, 1996.
- [5] P. Feldmann and J. Roychowdhury, "Computation of circuit waveform envelopes using an efficient, matrix-decomposed harmonic balance algorithm," *Proc. ICCAD 96*, pp. 295-300, 1996.
- [6] J. Roychowdhury, "Efficient methods for simulating highly nonlinear multi-rate circuits," *Proc. DAC 97*, pp. 269-274, 1997.
- [7] H. Brachtendorf, "A novel time-frequency method for the simulation of the steady-state of circuits driven by multi-tone signals," *Proc. ISCAS 97*, pp. 1508-1511, 1997.
- [8] V. Rizzoli *et al.*, "Nonlinear processing of digitally modulated carriers by the inexact-Newton harmonic-balance technique," *Electron. Lett.* vol. 33, pp. 1760-1761, Oct. 1997.
- [9] V. Borich *et al.*, "A fixed-point harmonic balance approach for circuit simulation under modulated carrier excitation," *Proc. ISCAS 99.*, to appear.
- [10] J. Bussgang *et al.*, "Analysis of nonlinear systems with multiple inputs," *Proc. IEEE*, pp. 1088-1119, vol. 62, Aug. 1974.
- [11] S. A. Maas, *Nonlinear Microwave Circuits*. Norwood, MA: Artech House, 1988.
- [12] C. Van Loan, *Introduction to Scientific Computing*. Upper Saddle River, NJ: Prentice Hall, 1997.